

Letter**Equilibrium Sizes and Dynamics of Flexible Knots**Pik-Yin Lai^a*Department of Physics and Center for Complex Systems, National Central University,
Chung-Li, Taiwan 320, R.O.C.*

(Received January 3, 2002)

Topologically distinct knotted polymers in equilibrium under good solvent conditions are investigated by Monte Carlo simulations. The equilibrium sizes of the knots, relaxation times and self-diffusion coefficients are measured for different knot types and chain lengths. The equilibrium knot size and fast relaxation time can be understood in terms of a blob picture and some scaling results are derived which agree with the simulation data.

PACS. 61.41.+e – Polymers, elastomers, and plastics.

PACS. 83.10.Nn – Polymer dynamics.

PACS. 87.10.+e – General, theoretical, and mathematical biophysics.

I. Introduction

Due to the breakthrough of Jones polynomials [1] in knot theory, there has been much research interest in the connection between physics and knot theory [2, 3] in the last decade. On the other hand, the advances in recent experimental techniques which can manipulate naturally occurring knotted DNA [4-6], as well as artificially tying up a molecule into a knot [7], calls for some fundamental understanding of the physical properties of knotted chain molecules. It is clear that the topological constraint in a knotted molecule dictates the important physical and geometrical properties of the knot [8-14]. Since a detailed mathematical description of knots is not available yet, one is still far away from any detailed theory of the physical properties of knots; a scaling approach and computer simulations remain the most effective theoretical tools at present. The common nomenclature of a knot is denoted by C_K , where C is the number of essential crossings i.e. the minimum number of crossings on any planar projection no matter how one manipulates the knot without cutting it, and K is just a label to distinguish topologically different knots. Although C cannot distinguish different complex knots effectively, C is a convenient parameter to describe many physical properties of a knot, such as the mean crossing number [13] and non-equilibrium relaxation times [11, 14]. The notion of a maximally inflated knot (“ideal” knot) may be also useful in some contexts [10]. Grosberg *et al.* [9] introduced a topological invariant ρ defined as the aspect ratio of the contour length (L) to the diameter (d) of a knotted polymer at its maximum inflated state, $\rho = L/d$. ρ can distinguish different knot types somewhat better than C , but on average ρ varies linearly with C .

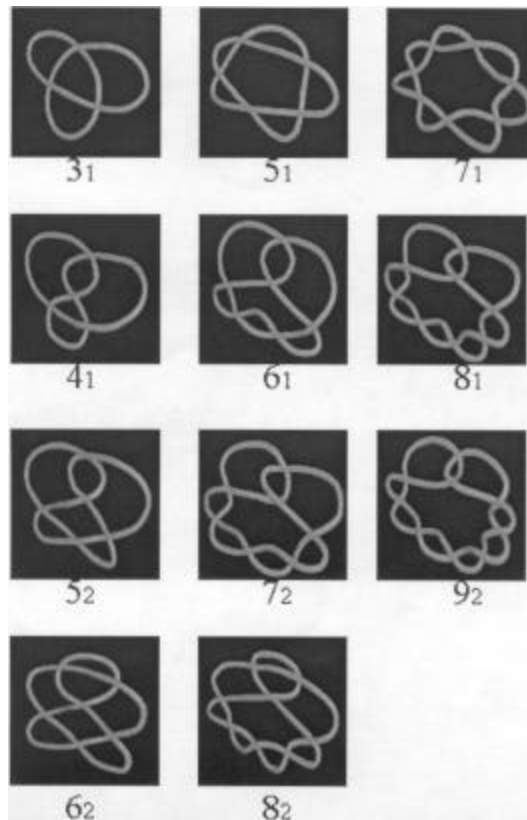


FIG. 1. Knot diagrams for various prime knots.

Dynamic Monte Carlo simulations using the bond-fluctuation model [15, 16] are employed in this study. There are only two basic interactions in our model: the first is the excluded volume effects between the monomers which can be thought of as a knot having a finite cross-section thickness; the second being the prohibition of any segment crossing in the course of the dynamics. It is clear that the latter interaction is of strong topological nature which guarantees that the initial knot type will remain the same. Different prime knots up to 20 essential crossings, with number of monomers up to $N = 240$, are investigated. The equilibrium mean square radii of gyration (R_g) and dynamical properties of four homologous knot groups (see Fig. 1) namely the torus knots ($3_1; 5_1; 7_1; \dots$), the even twist knots ($4_1; 6_1; 8_1; \dots$), the odd twist knots ($5_2; 7_2; 9_2; \dots$) and the ($6_2; 8_2; 10_2; \dots$) group are investigated in this work. These knots have been shown to classify into the above four groups in terms of their non-equilibrium relaxation times [11, 14]. Exploiting the idea that the topological constraint of forbidding chain segments to cross gives rise to “topological excluded volume interactions”, a trivial knot (unknot) of g -segments has an topological excluded volume of $\gg g^\circ$, where \circ is the self-avoiding exponent in three-dimensions. \circ is taken to be $\circ = 3/5$ throughout the analysis. Consider a non-trivial prime knot of N monomers with C essential crossings, on average the first monomer will be close to the $(N=C)^{\text{th}}$ monomer due to the topological constraints and hence can be modelled as a blob of $N=C$ segments. Applying the

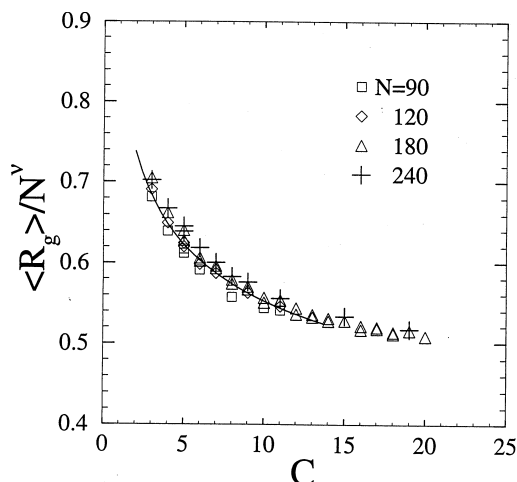


FIG. 2. Scaling plot of $\langle R_g \rangle / N^\nu$ versus C for the various prime knots with different chain lengths. The solid curve denotes a $C^{-4/15}$ behavior for small C

scaling concept of the blob picture in polymer physics, the length scale of the blob size is then set to be $\gg (N=C)^\nu$, provided that $N=C \gg 1$. The average number of blobs is C . If C is not much larger than 1, then the ring of blobs will fill the knot in a more or less compact way, i.e. with the volume of the knot $\gg R_g^3 \approx C \gg 1$, and hence one has $R_g \approx N^\nu C^{1/3} \approx N^{3/5} C^{1/15}$ which is exactly the result derived by Quake [8] without using the blob picture. However, if the number of essential crossing is large, i.e. the number of blobs $C \gg 1$ (but $C \ll N$ still holds), the chain of blobs can be viewed as a self-avoiding random walk forming a ring, which is not spacing filling. As a result, the knot size is given by the characteristic size of a ring of self-avoiding random walk of C blobs, $R_g \approx C^\nu \gg N^\nu$, which is independent of C . The above two scaling limits can be put into the following scaling form $R_g = N^\nu f(C)$, where $f(C) \gg \text{constant}$ for $C \gg 1$ and $\approx C^{-4/15}$ for $C \gg O(1)$. It should be noted that the above scaling results hold when the number of monomers inside a blob, $N=C$, is $\gg 1$, i.e. the knot is far from being tight. The scaling plot (Fig. 2) displays a good data collapse and agreement with the form of $f(C)$. A crossover scaling behavior is clearly observed as C increases, $\langle R_g \rangle$ becomes extremely slowly varying with C for $C > 15$, although much larger value of C are needed to verify firmly that $f(C)$ indeed approaches a constant. Our data do not agree with the recent result by Grosberg [17] for $C \gg 1$, which suggests $R_g \approx N^{3/5} C^{4/15}$ for knots with excluded volume. Since p varies linearly with C , this would imply the decrease in $R \approx C^{-4/15}$, which is consistent with our simulation data only for small C .

To monitor the relaxation dynamics in our simulations, the time auto-correlation of the radius of gyration, $\langle (R_g(t)R_g(0)) \rangle = \langle (R_g^2(t) - \langle R_g^2 \rangle) (R_g^2(0) - \langle R_g^2 \rangle) \rangle$ is measured. In general, non-trivial knots with higher values of C decay faster. For non-trivial knots with small values of C (such as $3_1, 4_1$), their initial relaxation behavior is close to that of the unknot, however all non-trivial knots show a long time tail in their correlation functions [18]. The faster relaxation time scale can be measured accurately by the half-decay time $\tau_{1/2}$, which is defined as the time needed for the correlation function to decay to $1/2$. Our data for the fast relaxation time $\tau_{1/2}$ do not agree with the

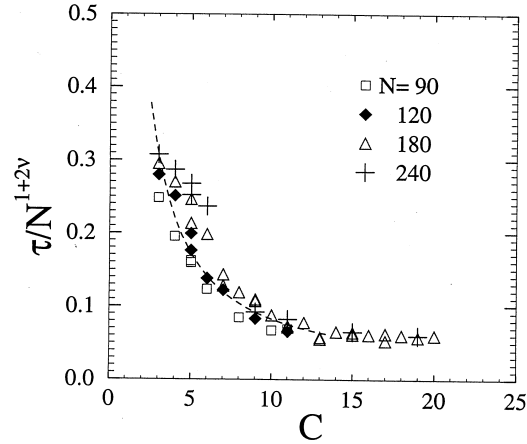


FIG. 3. Scaling plot of τ/N^{1+2° versus C . The dashed curve shows a $\tau \propto C^{i^{2^\circ}}$ behavior. $\circ = 0.6$.

scaling result by Quake [8], which predicted the relaxation time scales as $\tau = N^{1+2^\circ} \propto C^{2-3i^{2^\circ}} \propto C^{i^{0.533}}$. The decrease of τ with C is much stronger (as compared with [8]) for small values of C and seems to crossover to some much slower decrease for larger values of C . Furthermore, this scaling exponent in C was also not satisfactorily verified by the simulation data in Ref. [8], in which knots up to 10 crossings were studied and a fast relaxation time was fitted with a variation of $\tau \propto C^{i^{0.7}}$. The general trend of decreasing relaxation times with C indicates that more complex knots respond faster. This is due to the fact that more complex knots are in general more compact and possess stiffer elastic behavior. The latter properties have also been observed in our recent simulation studies [12] on the deformation of polymer knots. Based on the same blob picture, the relaxation time within a blob scales as $\tau_b \propto (N=C)^{1+2^\circ}$, and for $C \gg 1$, the relaxation of the whole knot can be viewed as relaxation of C self-avoiding blobs; thus the time needed for the relaxation to cover a region composed of a self-avoiding walk of C blobs is $\tau \propto C^{1+2^\circ} \tau_b \propto N^{1+2^\circ} \frac{1}{4} N^{\frac{11}{5}}$, for $C \gg 1$. On the other hand, for $C \gg O(1)$, the knot no longer has a configuration of a random walk of blobs but rather consists of a small number of blobs, then the time needed for the relaxation to propagate through the knot is of the order $\tau \propto C \tau_b \propto N^{1+2^\circ} C^{i^{2^\circ}} \frac{1}{4} N^{\frac{11}{5}} C^{i^{\frac{6}{5}}}$, which agrees with the initial fast decrease of τ with C . Again the above two scalings can be summarized in the following scaling form $\tau = N^{1+2^\circ} g(C)$, where $g(C) \propto \text{constant}$ for $C \gg 1$ and $\propto C^{i^{2^\circ}}$ for $C \gg O(1)$. Our scaling form is checked by our simulation data and the result is shown in Fig. 3. For $C > 10$, the data indeed settle to a constant while for smaller values of C , the data for different values of N do fall roughly as $\tau \propto 1=C^{1.2}$ (dashed curve). There is some scattering in the scaled data, which is probably due to the correction of finite- N in the exponent in N . The fast relaxation time scale is basically due to the elastic response of the knot. The extra elasticity of the knotted polymer, as compared to the free linear polymer, is given by the topological constraint of the knot, which is in turn provided by the excluded volume interactions and the entanglement effects among the chain segments. However, the increase in excluded volume interactions in a knot arises fundamentally from the topological constraint of maintaining the knot to be of the same type, which forces the polymer to remain strongly entangled.

Finally, the diffusion transport dynamics of knotted polymers is studied by monitoring the mean-square displacement of the center-of-mass position (\overline{R}_{cm}) in our simulations. The mean-square displacement varies linearly with t , indicating a free diffusion behavior for both the unknot and non-trivial knots up to 20 crossings. The self-diffusion coefficient is extracted from the mean-square displacement data as $D = \lim_{t \rightarrow \infty} \frac{1}{t} [\overline{R}_{cm}(t) - \overline{R}_{cm}(0)]^2 = 6t$. D shows a general decreasing trend with increasing C . The values of D for different knots approach to the same value in the large N limit, thus the self-diffusion behavior follows the Rouse dynamics for knots in the asymptotic long chain limit [18]. The motion of monomers in a knot can be pictured as confined inside an imaginary inflated knotted tube, or the “ideal form” [10] of the knot. The diffusion coefficient of the knot can be calculated according to the Einstein relation: $D = k_B T / \zeta_t$ where $k_B T$ is the Boltzmann constant times temperature and ζ_t is the total friction coefficient. In the Rouse model [19], the friction coefficient is proportional to the number of monomers N in the macromolecule, i.e. $N \gg \zeta$, where ζ is the monomer-solvent friction coefficient. For a linear polymer chain, the monomers tend to avoid each other in good solvents and the probability of two monomers in direct close contact is small. However, for knotted polymers, monomers are forced to be in close contact because of the topological constraint. During the relaxation process, monomers will slide onto each other and extra friction results. The collision probability among the monomers is greatly increased as the number of crossings increases. Using an analog to electric resistance to estimate this internal friction [11], the monomer-monomer friction coefficient is assumed to be proportional to the ratio of length to cross-section area of the ideal inflated knot. Thus the total friction coefficient can be expressed as $\zeta_t = N \zeta + L^3 / \rho^3$, where ρ^3 represents the monomer-monomer friction coefficient and $\rho^3 = d^3 / \rho_0^2$ for some characteristic monomer-monomer friction ρ_0^2 . Following the idea of the construction of the maximally inflated tube, one has $L \gg R_g \rho^{2/3}$ and $d \gg R_g \rho^{1/3}$. Then $\zeta_t = N \zeta + \rho_0^2 N \rho^{8/5}$ and hence

$$\frac{k_B T}{D} = N \zeta + \frac{\rho^{4/3}}{R_g} \rho_0^2 \quad (1)$$

The values of ρ for various prime knots in their ideal inflated forms have been calculated in [6]. By fitting the values of ρ from [6] with C , we obtain $\rho = 3.78C + 6$ and the values of ρ for all the knots in this study are then calculated using this linear relation. Fig. 4 plots $1/DN$ against $\rho^{4/3} = (hR_g^2 / \rho) N$ for various prime knots with different lengths, and the data collapse rather well and agree with the scaling result in Eq. (1). One recovers the standard Rouse behavior of $D \gg 1/N$ in Eq. (1) for knots with $\rho \ll N$ (i.e. for knots with smaller values of C) which also agrees with the simulation data [18]. It is worth noting that the relation $\zeta \gg hR_g^2 / \rho = D$ does not hold for polymer knots and in general $\zeta < hR_g^2 / \rho = D$, as indicated by our simulation data. This is because ζ is the fast relaxation time of the knot which reflects the time scale of blob relaxation and global elastic response, while $hR_g^2 / \rho = D$ is the time scale originating from the frictional drag experienced by the knot segments, which has a stronger dependence on the detail topology and hence is in general slower than ζ .

Acknowledgments

This research is supported by National Council of Science of Taiwan under Grant No. NSC 90-2118-M-008-037.

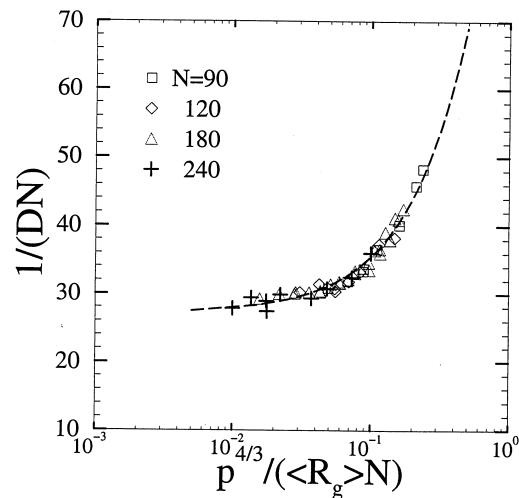


FIG. 4. A plot of $1/(DN)$ versus $p^{4-3} = (\langle R_g \rangle^3 / N)$ for various types of knots of different lengths. The dashed curve denotes the behavior given in Eq. (1). The x-axis is in log-scale so as to show the data collapse clearly.

References

^aElectronic address: pylai@phy.ncu.edu.tw

- [1] V. F. R. Jones, *Bull. Am. Math. Soc.* **12**, 103 (1985).
- [2] F. Y. Wu, *Rev. Mod. Phys.* **64**, 1099 (1992).
- [3] L. H. Kauffman, *Knots and Physics, 2nd edition* (World Scientific, Singapore 1993).
- [4] W. R. Bauer, F. H. C. Crick and J. H. White, *Scientific America* **243**, 118 (1980).
- [5] S. A. Wasserman and N. R. Cozzarelli, *Science* **232**, 951 (1986).
- [6] A. Stasiak, V. Katritch, J. Bednar, D. Michoud, and J. Dubochet, *Nature*, **384**, 122 (1996).
- [7] Y. Arai, R. Yasuda, K.-I. Akashi, Y. Harada, H. Miyata, K. Kinoshita Jr. and H. Itoh, *Nature* **399**, 446 (1999).
- [8] S. R. Quake, *Phys. Rev. Lett.* **73**, 3317 (1994).
- [9] A. Yu. Grosberg, A. Feigel and Y. Rabin, *Phys. Rev. E* **54**, 6618 (1996).
- [10] A. Stasiak, V. Katritch and L. H. Kauffman (eds.), *Ideal Knots* (World Scientific, Singapore 1998).
- [11] Y.-J. Sheng, P.-Y. Lai and H.-K. Tsao, *Phys. Rev. E* **58**, R1222 (1998); *Physica A* **281**, 381 (2000).
- [12] Y.-J. Sheng, P.-Y. Lai and H.-K. Tsao, *Phys. Rev. E* **61**, 2895 (2000).
- [13] J.-Y. Huang and P.-Y. Lai, *Phys. Rev. E* **63**, 021506 (2001).
- [14] P.-Y. Lai, Y.-J. Sheng, and H.-K. Tsao, *Phys. Rev. Lett.* **87**, 175503 (2001).
- [15] I. Carmesin and K. Kremer, *Macromolecules* **21**, 2819 (1988); *J. Phys. (Paris)* **51**, 915 (1990).
- [16] P. Y. Lai, *Chin. J. Phys.* **36**, 494 (1998).
- [17] A. Yu. Grosberg, *Phys. Rev. Lett.* **85**, 3858 (2001).
- [18] P.-Y. Lai, "Dynamics of Polymer Knots at Equilibrium", preprint.
- [19] P. G. de Gennes, *Scaling Concepts in Polymer Physics* (Cornell University Press, Ithaca, NY, 1979).